THE JOURNAL OF BIOLOGICAL CHEMISTRY VOL. 285, NO. 6, pp. 4213–4223, February 5, 2010

Cell-Cell Contact Formation Governs Ca^{2+} Signaling by TRPC4 in the Vascular Endothelium

*EVIDENCE FOR A REGULATORY TRPC4-β-CATENIN INTERACTION**

Received for publication, August 27, 2009, and in revised form, November 27, 2009 Published, JBC Papers in Press, December 8, 2009, DOI 10.1074/jbc.M109.060301

Annarita Graziani[‡], Michael Poteser[‡], Wolfgang-Moritz Heupel[§], Hannes Schleifer[‡], Martin Krenn[‡], Detlev Drenckhahn[§], Christoph Romanin[¶], Werner Baumgartner[‖], and Klaus Groschner[‡1]

From the [‡]Institute of Pharmaceutical Sciences-Pharmacology and Toxicology, University of Graz, Universitätsplatz 2, 8010 Graz, Austria, the [§]Institute of Anatomy and Cell Biology, University of Würzburg, Koellikerstrasse 6, 97070 Würzburg, Germany, the [¶]Institute of Biophysics, University of Linz, A-4040 Linz, Austria, and the [‖]Department of Cellular Neurobionics, Institute of Biology II, RWTH-Aachen University, Kopernikusstrasse 16, 52056 Aachen, Germany

TRPC4 is well recognized as a prominent cation channel in the vascular endothelium, but its contribution to agonist-induced endothelial Ca^{2+} entry is still a matter of controversy. Here we report that the cellular targeting and Ca^{2+} signaling function of TRPC4 is determined by the state of cell-cell adhesions during endothelial phenotype transitions. TRPC4 surface expression in human microvascular endothelial cells (HMEC-1) increased with the formation of cell-cell contacts. Epidermal growth factor recruited TRPC4 into the plasma membrane of proliferating cells but initiated retrieval of TRPC4 from the plasma membrane in quiescent, barrier-forming cells. Epidermal growth factor-induced Ca^{2+} entry was strongly promoted by the formation of cell-cell contacts, and both siRNA and dominant negative knockdown experiments revealed that TRPC4 mediates stimulated Ca^{2+} entry exclusively in proliferating clusters that form immature cell-cell contacts. TRPC4 co-precipitated with the junctional proteins β-catenin and VE-cadherin. Analysis of cellular localization of fluorescent fusion proteins provided further evidence for recruitment of TRPC4 into junctional complexes. Analysis of TRPC4 function in the HEK293 expression system identified β-catenin as a signaling molecule that enables cell-cell contact-dependent promotion of TRPC4 function. Our results place TRPC4 as a Ca^{2+} entry channel that is regulated by cell-cell contact formation and interaction with β-catenin. TRPC4 is suggested to serve stimulated Ca^{2+} entry in a specific endothelial state during the transition from a proliferating to a quiescent phenotype. Thus, TRPC4 may adopt divergent, as yet unappreciated functions in endothelial Ca^{2+} homeostasis and emerges as a potential key player in endothelial phenotype switching and tuning of cellular growth factor signaling.

Channels formed by the canonical transient receptor potential protein 4 (TRPC4) are expressed in endothelial cells and have repeatedly been suggested as key determinants of endothelial Ca^{2+} signaling and of endothelial functions, such as nitric oxide release and barrier stability (1–4). However, this concept was very recently questioned by the results of siRNA[2] knockdown experiments in human macrovascular endothelial cells (5), which argued against a prominent role of TRPC4 in endothelial Ca^{2+} signaling. Nonetheless, these authors confirmed a key role of TRPC4 as a determinant of endothelial proliferation. TRPC4 is a signaling molecule that is tightly associated with the actin cytoskeleton involving a C-terminal PDZ interaction domain, which determines membrane recruitment and cellular targeting of functional channels (6). Importantly, besides its controversial role as an endothelial Ca^{2+} channel, TRPC4 has repeatedly been demonstrated to govern integrity of cell-cell junction, barrier function, and thus endothelial phenotype (3, 4).

Depending on cell culture conditions, endothelial cells can adopt either a fibroblastoid, proliferative phenotype or, upon formation of cell-cell adhesions, the typical quiescent, epithelioid phenotype. This quiescent endothelial cell layer displays tight and adherens junctions, the latter providing adhesive strength necessary for holding cells physically together and allowing tight junctions to form and maintain (7, 8). Cell-cell contact formation determines barrier function, inhibits endothelial proliferation (9), and has been recognized to govern the molecular organization of membrane-associated signaling complexes. Adhesion contacts between endothelial cells are mainly mediated by a vascular endothelium-specific member of Ca^{2+}-dependent adhesion molecules, VE-cadherin, which, like other classical cadherins, contains a cytoplasmic domain that is linked via catenin-type adaptor molecules to the cellular actin filament cytoskeleton (10, 11). Both VE cadherin as well as β-catenin represent not only key components of endothelial junctional complexes and determinants of barrier function but also essential signaling molecules involved in "outside-in" signal transfer and a key determinant of endothelial proliferation and fate (12, 13). We hypothesized that such adhesion-mediated changes in the endothelial signaling network may interfere with TRPC4 function and set out to comparatively analyze cellular localization and function of TRPC4 in the absence and presence of cell-cell adhesion contacts. We report herein that

* This work was supported by FWF (Austrian Science Fund) Projects P19820 (to K. G.), P18475 (to M. P.), and P18169 (to C. R.).
⌘ *Author's Choice*—Final version full access.
[1] To whom correspondence should be addressed. Tel.: 43-316-380-570; Fax: 43-316-380-9890; E-mail: klaus.groschner@uni-graz.at.

[2] The abbreviations used are: siRNA, small interfering RNA; EGF, epidermal growth factor; PBS, phosphate-buffered saline; GFP, green fluorescent protein; FRET, fluorescence resonance energy transfer; CFP, cyan fluorescent protein; YFP, yellow fluorescent protein.

the formation of cell-cell adhesions promotes recruitment of endothelial TRPC4 into plasma membrane complexes at cell-cell junctions and enables growth factor-dependent membrane presentation and Ca^{2+} entry through endothelial TRPC4 channels. Our results provide evidence for association of TRPC4 with junctional proteins and phenotype-dependent contribution of this cation channel to endothelial Ca^{2+} homeostasis.

MATERIALS AND METHODS

Cell Culture and Transfection—HMEC-1 cells (human microvascular endothelial cells) were kindly provided by Dr. F. Candal (Centers for Disease Control and Prevention, Atlanta, GA). HMEC-1 were cultured in MCDB131 (Invitrogen) containing 15% fetal calf serum (PAA, Pasching, Austria), 10 ng/ml EGF (BD Biosciences), and 1 mg/ml hydrocortisone (Sigma). HEK293 cells (wild type) were cultured in Dulbecco's modified Eagle's medium (Sigma) containing 10% fetal calf serum. HEK293 cells stably transfected with mTRPC4α (T4-60) were cultured in Dulbecco's modified Eagle's medium plus 0.25 g/liter Geneticin (G418, Invitrogen). Transient transfections of DNA constructs and siRNA were performed either with Fugene6 (Roche Applied Science) for transfection of HMEC-1 cells or with Transfast transfection reagent (Promega) according to the manufacturer's instructions.

DNA Constructs and Vectors—HEK293 or HMEC-1 cells have been transiently transfected with mTRPC4β (in pECFP-C1), either alone or in combination with GFP-β-catenin (in pEGFP-C1), kindly provided by R. M. Kypta (University College London) (19), or YFP-VE-cadherin (as C-terminally YFP-tagged fusion protein cloned into pcDNA3) (14). As a functional dominant negative form of TRPC4β (DNTRPC4), the truncated protein mTRPC4β-(1–292) (15) was used in calcium imaging experiments. Control transfections were performed using the pEYFP-C1 vector.

siRNA—siRNA sequences were GGAAG AGGAU GUGGA UACC (siTRPC4, according to Ref. 5) and AGGUA GUGUA AUCGC CUUG (scrambled). The 19-mers were synthesized 5′-FAM (carboxyfluorescein)-labeled (Eurofins MWG GmbH, Ebersberg, Germany). For knockdown experiments, 1.5 μg of siRNA was transfected according to the manufacturer's protocol. For control experiments, cells were transected with a similar amount of scrambled RNA.

Measurement of Transendothelial Resistance (TER)—Transwell plates (Corning Glass) with 6.5-mm diameter inserts and 0.5-μm pore size were coated with poly-L-lysine (Sigma). HMEC-1 cells were seeded with a density of 30,000 cells/well in parallel and in similar culture conditions as for biochemical experiments. TER was measured on subsequent days using the End-Ohm apparatus (World Precision Instruments, Sarasota, FL). Resistance readings from blank poly-L-lysine-coated filters were subtracted from the readings from filters seeded with cells, and the difference was multiplied by the area (0.24 cm^2). TER measurements were used to define cell culture conditions in terms of the prevailing endothelial phenotype (*i.e.* either proliferating cells that largely lack mature cell-cell adhesions, designated as the "subconfluent" state, and/or quiescent cells with established barrier function, designated as the "confluent state").

Biotinylation of Cell Surface Membrane Proteins—HMEC-1 cells were grown until they reached either 70% of confluence (subconfluent contact state) or until they formed a monolayer (confluent state) and preincubated for 20 min in serum-free MCDB131 in the presence or absence of EGF (100 ng/ml). The cells were washed twice with ice-cold PBS containing 1 mM $MgCl_2$, 0.8 mM $CaCl_2$ (DPBS, pH 8) and incubated on ice for 30 min with 0.5 mg/ml EZ-Link sulfosuccinimidyl 2-(biotinamido)-ethyl-1,3-dithiopropionate (Pierce) in DPBS. Washing the cells three times with ice-cold DPBS containing 10 mM glycine terminated the biotinylation reaction. Cells were then washed twice with ice-cold PBS, scraped off from the dishes in PBS, and centrifuged at 4 °C. The pellets were resuspended in 0.5 ml of ice-cold lysis buffer (Protein Prep Kit, Qiagen, Mississauga, Canada) according to the manufacturer's instructions. Biotinylated proteins (500 μg) were isolated by adding to cell lysates 60 μl of streptavidin beads (Pierce) in a total volume of 0.5 ml of PBS. The reaction tube was gently rotated end over end overnight at 4 °C. The beads were recovered by centrifugation for 5 min at 1000 $\times$ *g*, and the pellets were washed three times with ice-cold PBS containing 1% Triton X-100. The biotinylated cell surface proteins were eluted from the streptavidin-agarose beads in 60 μl of 2$\times$ Laemmli buffer, boiled at 95 °C for 5 min, and subjected to SDS-PAGE.

Immunoprecipitation and Western Blot—Cell lysates from HMEC-1 were obtained as described above. HEK293 and T4-60 cells were transiently transfected with β-catenin-GFP or VE-cadherin-YFP. 48 h after the transfection procedure, proteins from cell lysates (500 mg) were suspended in a total volume of 0.5 ml of PBS, preincubated with 50 μl of either protein A- or protein G-Sepharose beads (Pierce), and gently rotated for 1 h at 4 °C to remove nonspecific bound proteins. Precleared supernatants were incubated with 3 μg of antibody against either β-catenin, VE-cadherin, or GFP overnight at 4 °C under rotation. Subsequently, 50 μl of either protein A- or protein G-Sepharose beads were added to the immune complex for 2 h at room temperature. The beads were pelleted, washed three times with ice-cold PBS containing 1% Triton, resuspended in 50 μl of 2$\times$ Laemmli buffer, and heated to 95 °C for 5 min. Proteins from cell lysates, biotinylated samples, and immunocomplexes were separated by SDS-PAGE and transferred to nitrocellulose sheets using the iBLOT dry blotting system (Invitrogen).

Nitrocellulose membranes were treated with polyclonal antibody either against TRPC4 (1:200; Alomone Laboratories, Israel or alternatively an anti-TRPC4 antibody kindly provided by V. Flockerzi) or antibody against GFP (1:1000; Roche Applied Science) according to the manufacturer's instructions. After washing with PBS containing 0.1% Tween, membranes were incubated with horseradish peroxidase-conjugated secondary antibodies (1:5000, 1 h). Membranes were detected via Chemi Glow West detection system and developed using a Herolab RH-5.2 dark room hood, equipped with an E.A.S.Y 1.3 HC camera (Herolab GmbH, Wiesloch, Germany).

Immunocytochemistry—HMEC-1 cells were grown on coverslips in different densities. Adherent cells were washed twice with PBS and then fixed for 10 min in a solution containing 6.5 g/liter Na_2HPO_4, 4 g/liter NaH_2PO_4, 7% methanol, and 37%

formalin at pH 7.0. After three washing steps, cells were incubated with rabbit anti-TRPC4 antibody (Alomone) in the presence of 5% goat serum for 6 h. Cells were washed again and incubated with anti-rabbit fluorescein isothiocyanate-conjugated secondary antibody for 1 h. For staining of nuclei, cells were incubated with 1 mg/ml 4′,6-diamidino-2-phenylindole (Molecular Probes, Inc., Eugene, OR) for 5 min in methanol.

Measurement of Intracellular Ca^{2+}—HMEC-1 or HEK293 cells were grown on coverslips, transiently transfected either with pEYFP-C1 vector or pEYFP-C1-mTRPC4β-(1–292) as described above, until they reached either the subconfluent or confluent state.

Cells were loaded with fura-2/AM or fluo-3 in Opti-MEM medium (Invitrogen), washed, and constantly perfused throughout experiments with buffer containing 137 mM NaCl, 5.4 mM KCl, 10 mM HEPES, 10 mM glucose, 1 mM $MgCl_2$, pH 7.4 (nominally Ca^{2+}-free) or supplemented with 2 mM $CaCl_2$. For some experiments, HMEC-1 cells were preincubated for 20 min in MCDB131-free serum in the presence or absence of EGF (100 ng/ml).

Thrombin stimulation of HEK293 cells was performed by incubation of cells for 5 min in nominally Ca^{2+}-free solution. Ca^{2+} entry was typically initiated by elevation of extracellular Ca^{2+} subsequently to cell stimulation. Ca^{2+}-sensitive fura-2/AM fluorescence was measured ratiometrically at 340 and 380 nm excitation wavelength, and emission was collected at 510 nm. Digital image recordings were analyzed using Axon Imaging Workbench (Indec BioSystems, Santa Clara, CA).

Fluorescence Microscopy and Fluorescence Resonance Energy Transfer (FRET)—HEK293 cells were grown on polylysine-coated coverslips and transiently transfected with CFP-TRPC4 (donor), GFP-β-catenin (acceptor), or VE-cadherin-YFP (acceptor). A 488-nm solid-state laser and a 445-nm diode laser (Modu-Laser LLC, West Jordan, UT) were used for excitation. Because emission spectra of CFP- and GFP-labeled proteins showed a significant overlap, special calculations were performed to correct the images for the extended channel bleed-through (linear spectral unmixing (16)). Channel bleed-through at different image intensity (fluorophore abundance) values has been determined by analyzing cells transfected with only one of the two labeled proteins. The percentage bleed-through values were then used to calculate the normalized channel intensity on a pixel-per-pixel basis (17). A MultiSpec imager (Visitron Systems GmbH, Puchheim, Germany) was used for separating FRET images and was connected to a Photometrics CoolSNAP fx-HQ monochrome camera (Roper Scientific, Ottobrunn, Germany). This system was attached to an Axiovert 200M microscope (Carl Zeiss, Göttingen, Germany) in conjunction with a VisiChrome high speed polychromator (Visitron). Used filter sets (Chroma Technology Corp., Rockingham, VT) included a 485-nm cyan emission filter set (MultiSpec) and a 535-nm yellow emission filter set. MetaVue software (Universal Imaging Corp., Downingtown, PA) was used to acquire images and to control the system. Images were analyzed using MetaMorph (Universal Imaging) and ImageJ software (National Institutes of Health). As a measure of co-localization of the fluorescent proteins, the fraction (percentage) of pixels displaying overlap of the two fluorophores was determined for certain areas of interest (total cell, nuclear region, and contact area) using ImageJ software. FRET images have been corrected for "cross-talk." To achieve this, the corrected FRET image (FRET index) was calculated after background subtraction using the sensitized emission correction method according to the equation, FRET (index) = rawFRET − corrD*$I_{donator}$ − corrA*$I_{acceptor}$. The calibration factors were obtained from experiments where only CFP, YFP, or GFP was expressed (CFP, corrD = 0.42; YFP, corrA = 0.13; GFP, corrA = 0.54). Representative results from 14–19 FRET experiments have been selected for illustration.

RESULTS

Phenotype Transitions Govern Membrane Presentation of TRPC4 in HMEC-1—To investigate the impact of endothelial phenotype switching on membrane presentation of TRPC4 channels, surface biotinylation experiments were performed with human microvascular endothelial cells (HMEC-1). Surface expression of TRPC4 was clearly enhanced when cells formed cell-cell adhesions along with the transition from a proliferative ("subconfluent") to a quiescent barrier-forming ("confluent") state (Fig. 1*A*), displaying a maximum level of transendothelial resistance (Fig. 1*B*). Although a small overlap in terms of phenotype heterogeneity of both subconfluent and confluent populations may exist, barrier function was considered to correlate reasonably well with prevalence of mature cell-cell adhesions. Interestingly, EGF stimulation affected membrane presentation of TRPC4 in subconfluent and confluent cells in an opposing manner (Fig. 1*A*). EGF promoted recruitment of TRPC4 into the membrane surface of subconfluent cells but initiated removal of TRPC4 immunoreactivity from the membrane of barrier-forming endothelial cells. Because alternative splicing of TRPC4 has been demonstrated, we performed a set of Western blot experiments using an antibody provided by V. Flockerzi to elucidate the expression TRPC4 splice forms (18) in HMEC-1 and to obtain information on the relative contribution of the variants. These experiments suggested that the TRPC4 immunoreactivity observed in HMEC-1 corresponds mainly to the short (β) variant of the channel protein (data not shown).

Formation of Cell-Cell Contacts Enables a Ca^{2+} Signaling Function for TRPC4 in HMEC-1—As a next step, we tested whether different stages during phenotype transition are associated with altered endothelial EGF-induced Ca^{2+} signaling. Fig. 2 illustrates Ca^{2+} signals obtained during Ca^{2+} readdition protocols. Basal Ca^{2+} entry into non-stimulated cells and in all endothelial phenotypes tested was negligible, as illustrated for subconfluent cells (Fig. 2). Importantly, in subconfluent populations, both single cells as well as proliferating clusters were present. Peak levels of intracellular Ca^{2+} obtained after Ca^{2+} readdition to EGF-stimulated cells were minute in single cells and highest in proliferating clusters, whereas confluent cells displayed rises in intracellular Ca^{2+} slightly smaller than that recorded in subconfluent proliferating cell aggregates. Consistent differences were detected by calculating the rate of rise in cellular Ca^{2+} levels initiated by Ca^{2+} readdition (Fig. 2*B*). Thus, the most prominent effect of phenotype switching was the substantial promotion of EGF-induced Ca^{2+} entry by the transi-

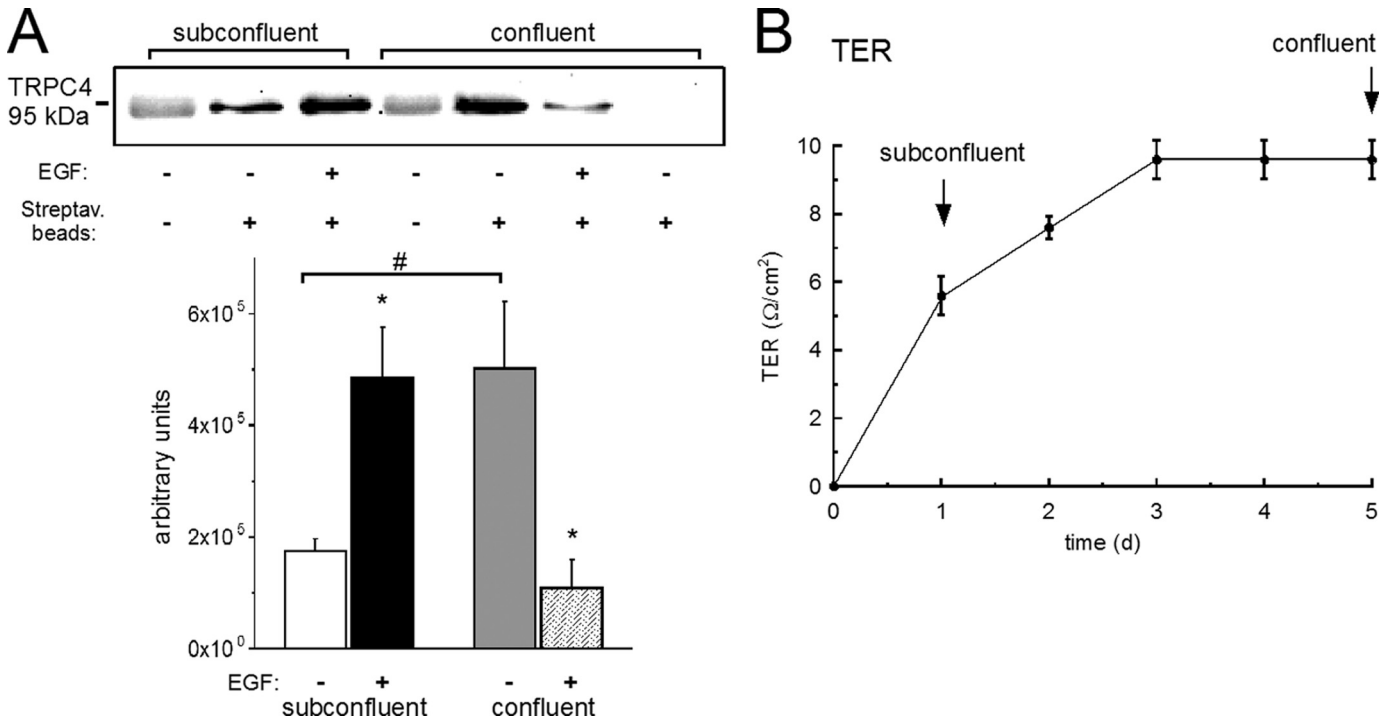

FIGURE 1. **Membrane presentation of TRPC4 is enhanced by formation of cell-cell contacts and divergently affected by EGF in subconfluent and confluent HMEC-1.** *A*, *top*, proteins from total cell lysates (*lanes 1* and *4*), biotinylated fractions (*lanes 2*, *3*, *5*, and *6*), and non-biotinylated fractions (*lane 7*) at the indicated conditions were subjected to SDS-PAGE and immunoblotted with TRPC4 antibody. Results are representative of four individual experiments. *Bottom*, mean values ± S.E. of TRPC4 immunoreactivity detected in biotinylated fractions before and after stimulation with EGF (100 ng/ml, 20 min). *, statistically significant differences between stimulated and unstimulated conditions ($p < 0.05$); #, statistically significant difference between the unstimulated subconfluent state and the unstimulated confluent state ($p < 0.05$). *B*, time course of TER increase in cultured HMEC-1 cells representing the transition from proliferating, subconfluent to barrier forming, confluent populations. TER levels (*arrows*) were taken as a basis to distinguish proliferating, subconfluent cells from mature barriers characterized by a constant, maximal TER level. The *trace* represents mean TER ± S.E. ($n = 6$). *d*, days.

tion from a single, contact-deficient phenotype to a state of proliferating cell clusters. Interestingly, the prominent Ca^{2+} entry signals observed in proliferating cell clusters were for a large part mediated by TRPC4, as indicated by siRNA silencing experiments (Fig. 2*A*, *inset*). Attempts to localize the TRPC4 protein by immunocytochemistry revealed an intracellular, rather polar distribution in single cells, whereas TRPC4 was symmetrically distributed with clearly detectable immunoreactivity within basolateral contact regions in proliferating cell aggregates as well as in confluent cell layers. Typical images are shown in Fig. 2*C*. Cell phenotype and cell-cell adhesions therefore determine not only membrane presentation of TRPC4 but also agonist-induced Ca^{2+} signaling in HMEC-1.

To further test the hypothesis of a phenotype- and cell contact-dependent contribution of TRPC4 to global Ca^{2+} homeostasis, we investigated the role of TRPC4 in cells of different phenotype by both dominant negative knockdown experiments and an siRNA knockdown approach. Contribution of TRPC4 channels to Ca^{2+} entry was tested by use of previously characterized dominant negative proteins (15). Based on the results shown in Figs. 1 and 2, we anticipated a contribution of TRPC4 signaling either in proliferating, contact-forming cells (subconfluent/contact) or in confluent, barrier-forming cells. Nonetheless, we started with characterization of the effect of dominant negative TRPC4 inhibition in single, contact-deficient HMEC-1 (Fig. 3*A*, *single*). Ca^{2+} entry measured in single EGF-stimulated HMEC-1 was minute and not affected by expression of dominant negative TRPC4. To test for a contribution of TRPC4 to stimulated Ca^{2+} entry into single cells at an elevated level, we used thrombin as an alternative agonist (Fig. 3*A*). With thrombin as an agonist, dominant negative TRPC4 again failed to inhibit Ca^{2+} entry into single HMEC-1, and overexpression of full-length TRPC4 also did not affect Ca^{2+} signals. Thus, when HMEC-1 cells reside in a cell-cell contact-deficient, migrating state, TRPC4 is barely detectable in plasma membrane regions and appears to lack Ca^{2+} signaling function. By contrast, the large Ca^{2+} entry signals measured in EGF-stimulated cells that formed immature contacts within proliferating cell clusters (Fig. 3*B*) were dramatically reduced by expression of a dominant negative TRPC4 protein or siRNA knockdown of TRPC4. Surprisingly, cells that adopted a barrier-forming, quiescent state exhibited Ca^{2+} entry that was barely sensitive to either TRPC4 knockdown strategy (Fig. 3*C*). Hence, suppression of TRPC4 function affected agonist-induced Ca^{2+} entry into HMEC-1 exclusively in proliferating cells that formed clusters and immature cell-cell adhesions. Contribution of TRPC4 to global endothelial Ca^{2+} signaling appears not to be simply correlated with the channel's membrane presentation but rather restricted to a specific state of endothelial cell-cell coupling and phenotype. These data indicated the existence of a membrane-targeted TRPC4 complex that is obtained by establishment of immature cell-cell adhesions in proliferating cell clusters and is capable of mediating EGF-induced Ca^{2+} entry.

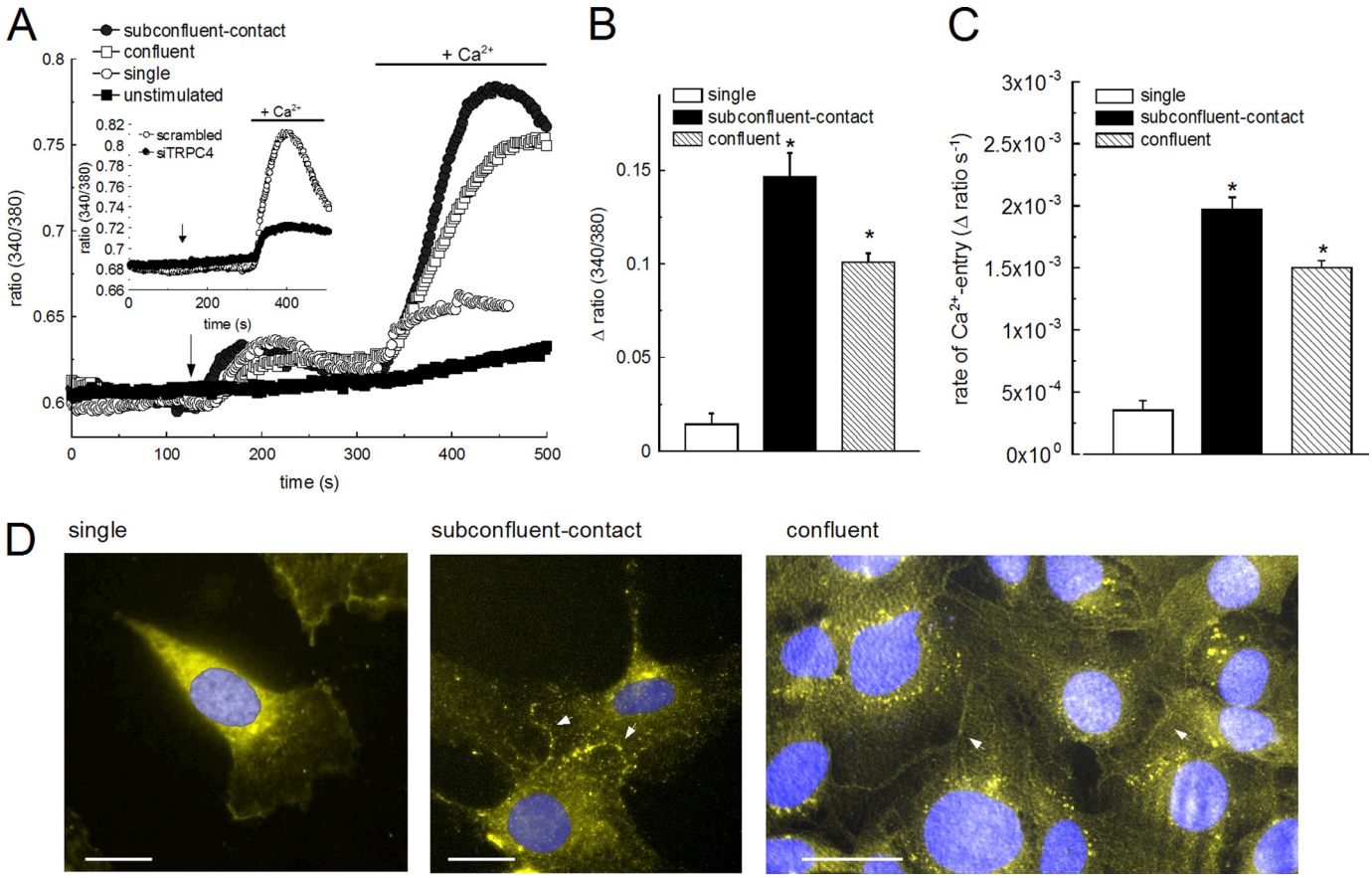

FIGURE 2. **EGF-induced Ca^{2+} entry is altered by endothelial phenotype transitions.** *A*, representative records of fura-2 fluorescence ratio in single (migrating state; *open circles*), subconfluent contact-forming (proliferating clusters; *closed circles*), and confluent (quiescent, barrier-forming; *squares*) cells during a Ca^{2+} readdition after stimulation with EGF (100 ng/ml; *arrow*). Ca^{2+} readdition (elevation of extracellular Ca^{2+} from nominally free to 2 mM) is indicated. Basal Ca^{2+} entry into non-stimulated cells is shown for proliferating clusters (unstimulated). The *inset* shows inhibition of Ca^{2+} entry into EGF-stimulated subconfluent cells by TRPC4 siRNA silencing. Responses of a TRPC4-silenced cell (*filled circles*) and a control (scrambled; *open circles*) are shown. *B*, mean peak increases in fura-2 emission ratios (Δ values ± S.E., $n \geq 45$) obtained during Ca^{2+} readdition. *C*, mean rates of Ca^{2+}-sensitive fluorescence changes during the initial phase of reentry. *, statistically significant difference ($p < 0.05$) *versus* the single, migrating phenotype. *D*, TRPC4 immunofluorescence images of single (migrating; *left*), subconfluent contact-forming (proliferating; *center*), and confluent (quiescent; *right*) HMEC-1 cells (nuclei stained by 4′,6-diamidino-2-phenylindole). The *arrows* indicate positions of enhanced TRPC4 immunofluorescence. *Scale bars*, 10 μm.

TRPC4 Associates with Components of Junctional Complexes in HMEC-1—We hypothesized that promotion of TRPC4 function in proliferating cell clusters may be based on the recruitment into specific signalplexes localized within immature adhesions. Hence, we next investigated the interactions of TRPC4 with junctional proteins. Co-immunoprecipitation experiments suggested association of TRPC4 with both VE-cadherin and β-catenin in HMEC-1. Fig. 4 shows the detection of TRPC4 in VE-cadherin and β-catenin precipitates from subconfluent as well as confluent HMEC-1 at basal and EGF-stimulated conditions. These experiments were performed with two different TRPC4 antibodies and yielded similar results. Association of TRPC4 with VE-cadherin was promoted by contact formation but diminished by EGF stimulation (Fig. 4*A*). Association with β-catenin was divergently regulated by EGF in subconfluent and confluent cells, respectively. As illustrated in Fig. 4*B*, interaction of TRPC4 with β-catenin was promoted by EGF stimulation in subconfluent cells but reduced in barrier-forming, confluent cells. Thus, not only membrane presentation and Ca^{2+} entry function of TRPC4 but also its interaction with junctional proteins and signalplex composition was determined by the endothelial phenotype. Because EGF stimulation of proliferating cells induced significant TRPC4-mediated Ca^{2+} entry along with profound TRPC4-β-catenin association, we considered β-catenin as a potential regulatory component of endothelial TRPC4 complexes.

TRPC4 Is Targeted into Cell-Cell Junctions and Co-localizes with Junctional Proteins in both HMEC-1 and HEK293 Cells—To further investigate cellular targeting of TRPC4 as well as of junctional proteins and to test for translocations associated with cell-cell contact formation, we performed fluorescence microscopy in cells transfected to express fluorescent fusion proteins of TRPC4 as well as of β-catenin and VE-cadherin. Because several attempts to generate suitable, properly targeted fusions of β-catenin with blue- or yellow-shifted GFP variants failed, we used the available GFP fusion along with a spectral unmixing approach (16). Fig. 5*A* illustrates the cellular localization of fluorescence-tagged TRPC4 (CFP) and β-catenin (GFP) when expressed individually in HMEC-1. Both proteins were barely targeted to the plasma membrane in single cells but tended to incorporate into cell-cell contacts upon cluster formation. Intracellular localization of the proteins was different, showing fairly uniform distribution for TRPC4 and a distinct pattern for β-catenin displaying fluorescence within nucleus-

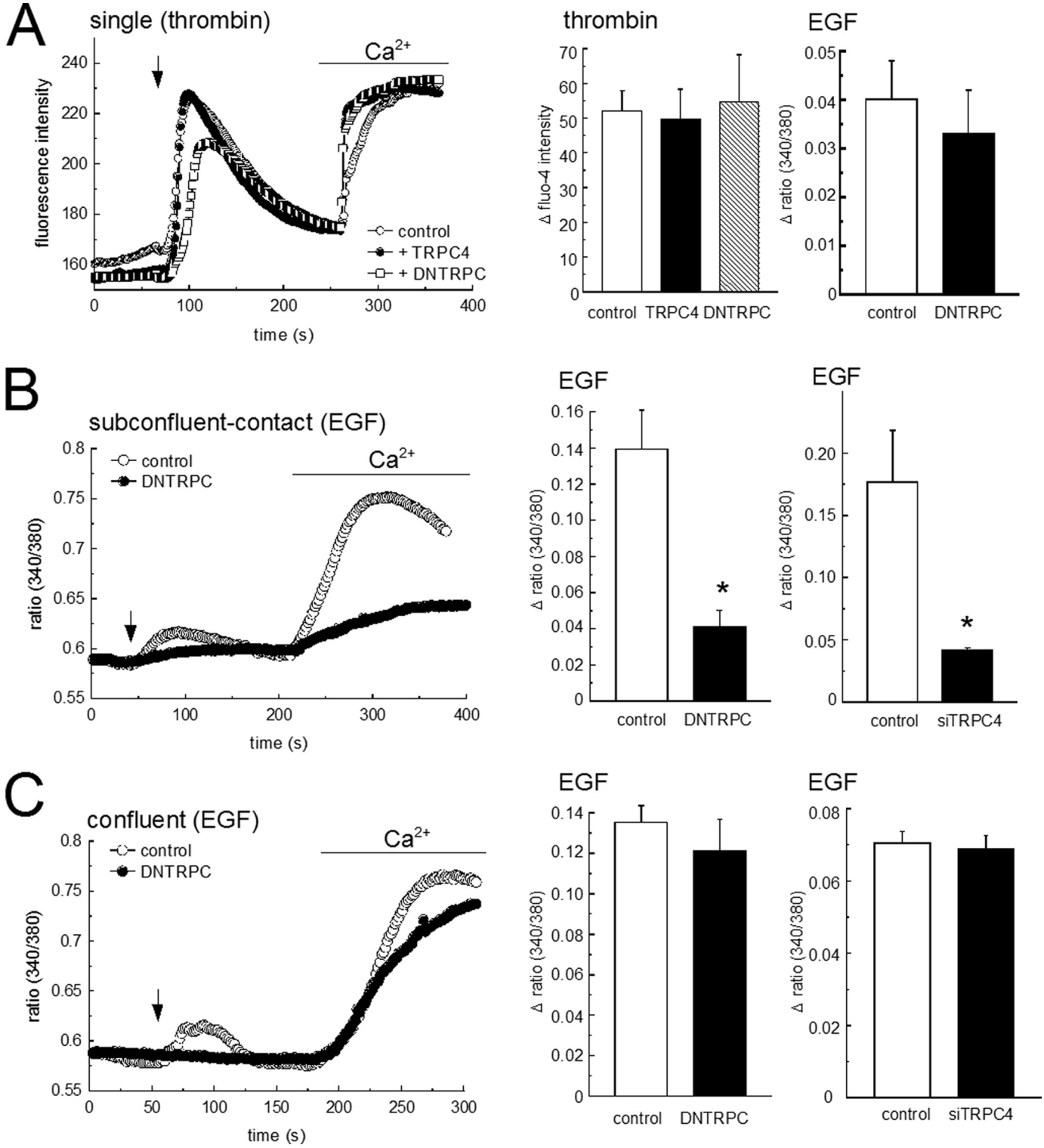

FIGURE 3. **Formation of immature cell-cell contacts in proliferating HMEC-1 enables TRPC4-dependent Ca^{2+} entry.** *A*, Ca^{2+} entry into thrombin or EGF-stimulated single HMEC-1 cells. *Left*, representative recordings of fluo-4 fluorescence intensity in single cells transfected with pcDNA3-vector (control; *open circles*), TRPC4 (*closed circles*), or a functional dominant negative TRPC4 fragment (DNTRPC; *squares*). Time courses during acute stimulation with 0.5 unit/ml thrombin (*arrow*) and Ca^{2+} readdition (2 mM) are shown. *Center*, mean values of peak fluo-4 intensity ($n > 6$; *open columns*, control; *hatched columns*, TRPC4; *filled columns*, DNTRPC). *Right*, mean increases in fura-2 fluorescence ratios ($n \geq 6$) obtained during Ca^{2+} readdition after stimulation with EGF (100 ng/ml). *B*, *left*, representative recordings of fura-2 fluorescence ratios in the subconfluent, contact-forming state is shown for controls (sham-transfected; *open circles*) and DNTRPC-transfected (*closed circles*) cells, HMEC-1 cells were challenged with EGF (100 ng/ml; *arrow*), as indicated. *Right*, increases in fura-2 fluorescence ratios (mean ± S.E.; $n \geq 8$). *C*, *left*, representative recordings of fura-2 fluorescence ratios in the confluent, barrier-forming state is shown for controls (sham-transfected; *open circles*) and DNTRPC-transfected (*closed circles*) cells, and HMEC-1 cells were challenged with EGF (100 ng/ml; *arrow*), as indicated. *Right*, increases in fura-2 fluorescence ratios (mean ± S.E.; $n \geq 8$).

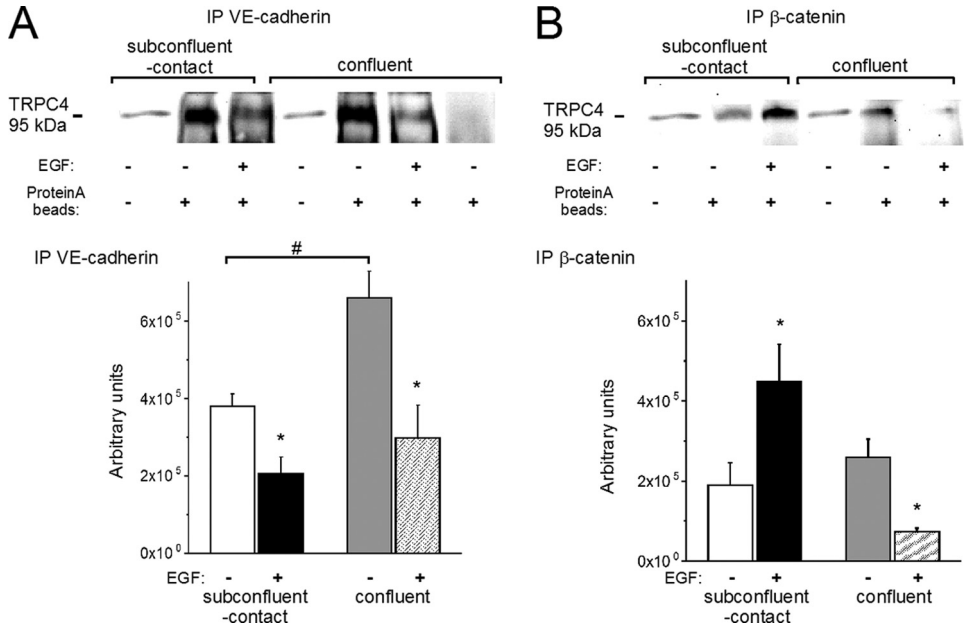

FIGURE 4. **Association of VE-cadherin and β-catenin with TRPC4 depends on cell-cell contact formation.** *A*, *top*, TRPC4 was detected in total cell lysates (from the *left*, *lanes 1* and *4*) immunocomplexes precipitated with anti-VE-cadherin (*lanes 2*, *3*, *5*, and *6*) and lysates precipitated only with beads (*lane 7*). Results are a representative of four experiments. *Bottom*, mean values ± S.E. of the TRPC4 immunoreactivity detected in precipitates obtained from cells before and after stimulation with EGF (100 ng/ml, 20 min). *B*, *top*, TRPC4 was detected in total cell lysates (from the *left*, *lanes 1* and *4*), immunocomplexes precipitated with anti-β-catenin (*lanes 2*, *3*, *5*, and *6*), and lysates precipitated only with beads (*lane 7*). Results are a representative of four experiments. *Bottom*, mean values ± S.E. of the TRPC4 immunoreactivity detected in precipitates obtained from cells before and after stimulation with EGF (100 ng/ml, 20 min). * and #, statistically significant differences ($p < 0.05$) between stimulated *versus* unstimulated cells and subconfluent state *versus* confluent state, respectively. *IP*, immunoprecipitation.

associated, rodlike structures, as previously reported (19, 20). Fig. 5*B* illustrates cellular targeting of TRPC4 and β-catenin in cells co-transfected to overexpress both proteins. In single, contact-deficient cells, the two proteins were found to co-localize within the intracellular compartment without detectable recruitment of the TRPC4 channel protein into the plasma membrane (Fig. 5*B*). In cell clusters, both CFP-TRPC4 and GFP-β-catenin were redistributed to co-localize within cell-cell contact areas. Plasma membrane recruitment of CFP-TRPC4 was observed exclusively in contact-forming cells and appeared to be enhanced by β-catenin overexpression. Acute EGF stimulation of clustered HMEC-1 failed to produce further detectable changes in membrane targeting of CFP-TRPC4 (not shown).

Because transfection rates of HMEC-1 were essentially low, we complemented our analysis of cellular localization and interaction of TRPC4 with junctional proteins by employing the HEK293 system, which allows efficient expression of fluorescent fusion proteins and has previously been proven useful in analyzing cell-cell coupling-dependent signaling mechanisms (21, 22) as well as TRPC function (23, 24). CFP-TRPC4 and GFP-β-catenin were found to localize in a similar manner as in HMEC-1, with the exception that TRPC4 was clearly visible in the plasma membrane of single HEK293 cells (Fig. 5*C*). In cells co-transfected with these fusion proteins, we observed a striking co-localization and a similar pattern of cellular distribution as in HMEC-1. Again the fluorescent proteins were predominantly detected in an intracellular compartment of single, contact-deficient cells but were targeted to cell-cell contact regions in HEK293 clusters. Recruitment of TRPC4 into cell-cell adhesions was barely observed without overexpression of β-catenin. In HEK293 cells, the impact of β-catenin on the cellular localization of TRPC4 in single cells was even more prominent than in HMEC-1. In contact-devoid HEK293 cells, β-catenin overexpression reduced membrane targeting of TRPC4 and induced retention of the channel within an intracellular compartment.

As a next step, we aimed to analyze targeting of TRPC4 into cell-cell contacts and its interaction with junctional proteins by FRET microscopy. As shown in Fig. 6*A*, TRPC4 not only co-localizes with β-catenin within cell-cell contacts, but the two proteins also associate in close proximity within junctional complexes, as evident from energy transfer. Similarly, we tested for co-localization of TRPC4 with VE-cadherin, representing another junctional interaction partner of TRPC4 in endothelial cells. Both co-localization and FRET analysis demonstrated that also YFP-VE-cadherin interacts with CFP-TRPC4 within cell-cell contacts of HEK293 cells (Fig. 6*B*). The interaction of TRPC4 with both β-catenin and VE-cadherin in the HEK293 expression system was also corroborated by immunoprecipitation (not shown).

β-Catenin Promotes the Ca^{2+} Signaling Function of TRPC4 in a Strictly Cell-Cell Adhesion-dependent Manner—Membrane targeting of β-catenin-TRPC4 complexes was detected in proliferating cell clusters, representing a state that was also characterized by significant contribution of the channel to overall Ca^{2+} signaling. This prompted us to investigate the impact of β-catenin on TRPC4 function.

Due to low transfection efficiency with HMEC-1, we again utilized the HEK293 expression system, which was found to display cell-cell contact-dependent targeting and interaction of TRPC4 with junctional proteins similar to HMEC-1. Expression of β-catenin in the stable TRPC4-expressing cell line T4-60 generated a profound cell adhesion-dependent increase in agonist-induced Ca^{2+} signaling. Fig. 7 illustrates that thrombin-induced Ca^{2+} entry was barely dependent on cell-cell contact formation in HEK293 wild type cells or vector-transfected T4-60 but markedly promoted by establishment of cell-cell adhesions in β-catenin-overexpressing T4-60 cells. β-Catenin failed to affect Ca^{2+} entry via endogenous pathways in HEK293 cells but remarkably promoted TRPC4-mediated Ca^{2+} entry when cells formed cell-cell adhesions. Overexpression of VE-cadherin resulted in only modest promotion of Ca^{2+} entry into contact-forming T4-60 cells. Thus, β-catenin emerges as a novel signaling partner of TRPC4 that enables cell adhesion-dependent Ca^{2+} signaling.

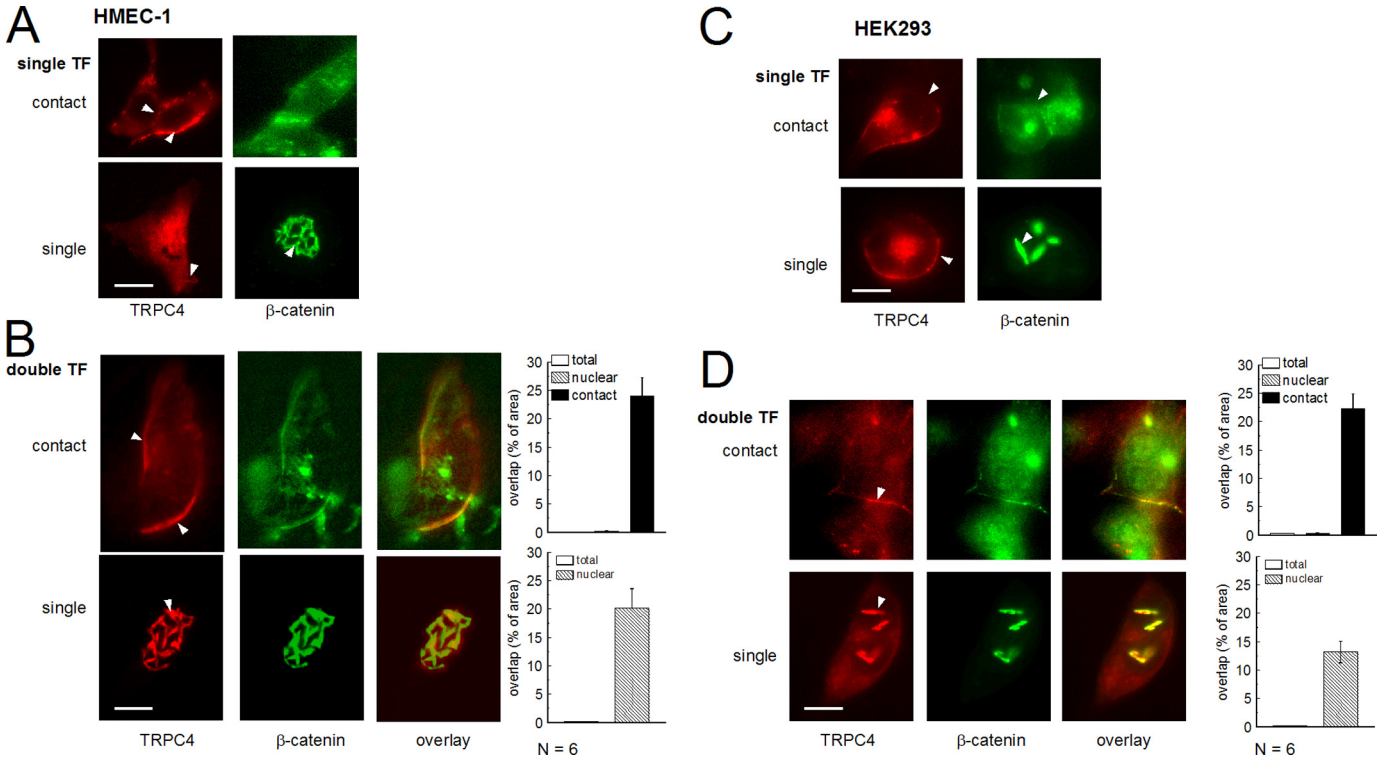

FIGURE 5. **Cell-cell contact formation and β-catenin expression determines the cellular targeting of TRPC4.** Fluorescence images of single (*top images*) or contact-forming (*bottom images*) HMEC-1 (*A* and *B*) and HEK293 (*C* and *D*) cells transfected with either CFP-TRPC4 (*red*) or GFP-β-catenin (*green*) alone (*A* and *C*) or double transfected with both constructs (*B* and *D*). The *arrows* indicate enhanced fluorescence of CFP-TRPC4 or GFP-β-catenin, respectively. *A*, fluorescence images of single transfected (*single TF*) HMEC-1 cells. *B*, fluorescence images of double transfected (*double TF*) HMEC-1 cells. *C*, fluorescence images of single transfected HEK293-cells. *D*, fluorescence images of double transfected HEK293 cells. Images from cells expressing GFP and CFP have been normalized for channel bleed-through by linear spectral unmixing. *Scale bars*, 10 μm. For *B* and *D*, relative values of fluorescence overlap as a measure for co-localization are shown for defined cellular regions (total cell, nuclear region, and cell-cell contact area). The *columns* represent the overlap of the two fluorophores (percentage of pixels) within selected cellular areas (mean ± S.E.).

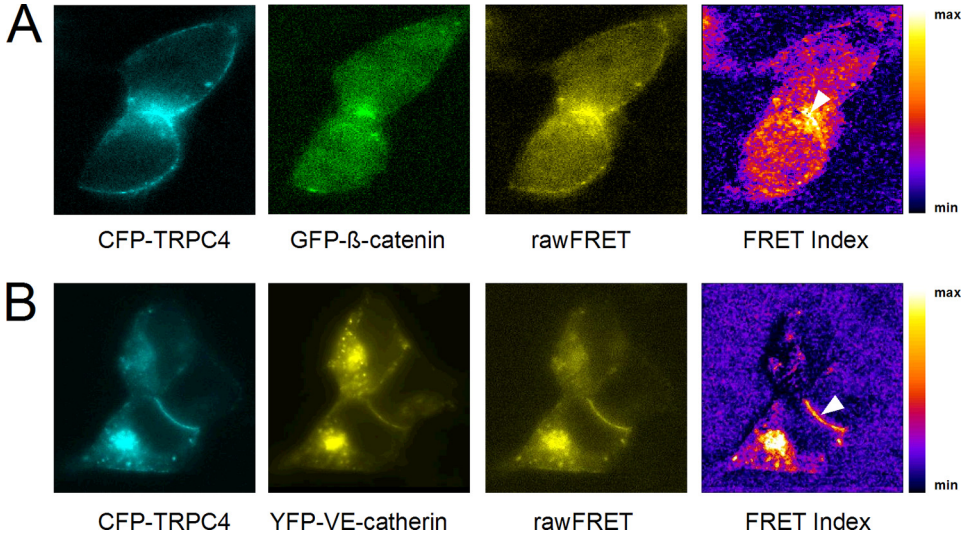

FIGURE 6. **Interaction between TRPC4 and VE-cadherin within cell-cell contacts in the HEK293 expression system.** This figure shows donor (CFP), acceptor (YFP), and raw FRET images as well as a *color-coded map* of FRET intensity (FRET index) after background subtraction. *A*, FRET analysis of CFP-TRPC4 and GFP-β-catenin transiently expressed in HEK293 cells. *B*, FRET analysis of CFP-TRPC4 and YFP-VE-cadherin transiently expressed in HEK293 cells. The *arrows* indicate enhanced FRET signal at cell-cell contact positions and cell-cell junctions. Images are representative of 14–19 individual FRET measurements.

DISCUSSION

This study introduces TRPC4 as an endothelial Ca^{2+} entry channel that is efficiently controlled by cell-cell contacts and interactions with junctional proteins. Our results support recent evidence arguing against a role of TRPC4 in terms of a general, prominent effector channel in the phospholipase C/store depletion pathway of endothelial cells (5). Moreover, we identify β-catenin as a regulator of TRPC4-mediated Ca^{2+} signaling. TRPC4 emerges as a specialized signaling molecule serving phenotype-dependent control of endothelial Ca^{2+} homeostasis and tuning of growth factor signaling.

Cellular Targeting of TRPC4 and Endothelial Ca^{2+} Signaling Is Dependent on Cell-Cell Contact Formation—Agonist-induced membrane recruitment of TRPC4 has repeatedly been demonstrated for vascular endothelium (25, 26). Here we show that surface targeting is dependent on cell-cell contact formation. Transition of endothelial cells from a proliferating into a quiescent, barrier-forming state was found to be associated with promotion of membrane insertion of TRPC4. Phenotype-dependent cellular targeting of TRPC4 was even more pronounced when cells were challenged with EGF. EGF evoked

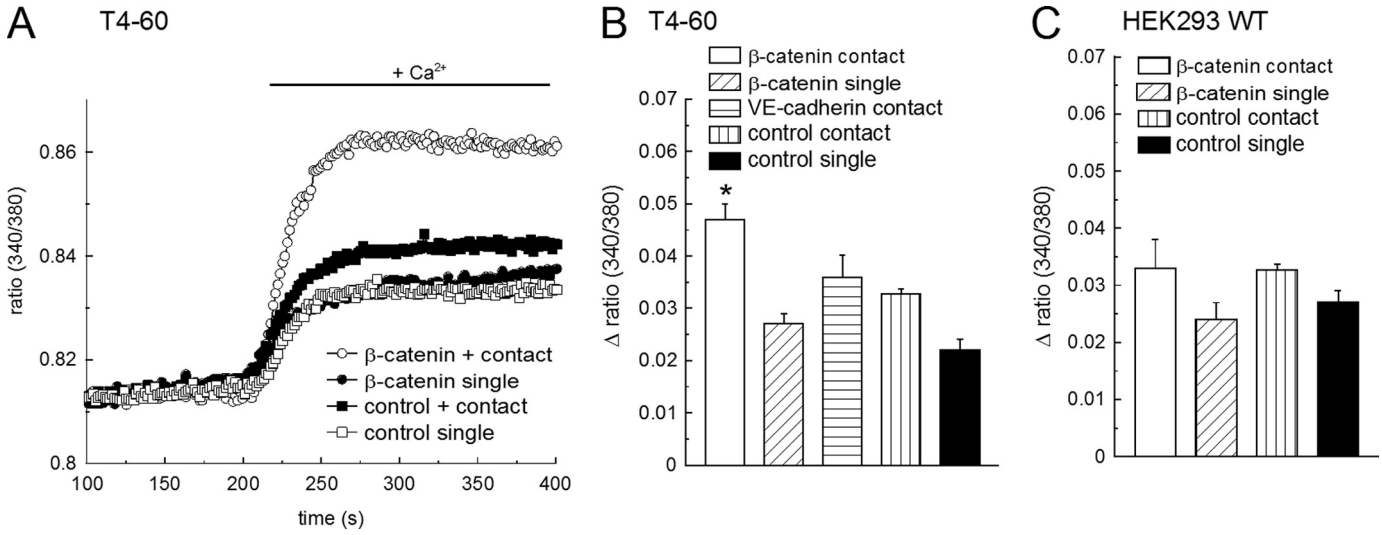

FIGURE 7. **β-catenin enables cell-cell contact-dependent promotion of Ca^{2+} entry into TRPC4-expressing HEK293 cells.** Ca^{2+} entry into thrombin-stimulated HEK293 cells during a typical Ca^{2+} readdition protocol. *A*, representative recordings of fura-2 fluorescence ratios from single or contact-forming HEK293 cells stably expressing TRPC4 (T4-60), transfected with either pcDNA3 (control) or β-catenin. Ca^{2+} readdition (from nominally free to 2 mM) was performed as indicated after a 5-min stimulation with thrombin (0.5 unit/ml; pretreatment). Shown are mean peak increases in fura-2 fluorescence ratios (Δ values $\pm$ S.E.) obtained during Ca^{2+} readdition to single or contact-forming T4-60 (*B*) as well as HEK293 cells (*C*). *, statistical significance ($p < 0.05$) *versus* contact-forming controls as well as single cells. *WT*, wild type.

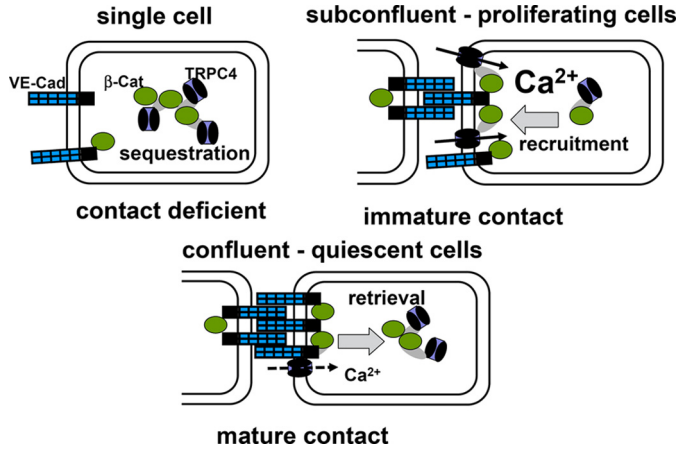

FIGURE 8. **Proposed model of phenotype-dependent TRPC4 function in growth factor-stimulated endothelial cells via interaction of the channel with β-catenin and targeting into cell-cell contacts.** TRPC4 is for a large part sequestered in intracellular compartments and unavailable for Ca^{2+} signaling in single cells (*contact deficient*; *upper left*). By contrast, formation of immature cell adhesions promotes surface targeting of β-catenin-TRPC4 complexes and enables further recruitment of channels into the plasma membrane and Ca^{2+} entry function (*immature contact*; *upper right*). Once mature barriers are formed (*mature contact*; *lower panel*), TRPC4 resides for a large part in junctional complexes that are rapidly retrieved from the cell surface during growth factor stimulation and are barely available for contribution to global Ca^{2+} signaling.

recruitment of TRPC4 into the plasma membrane of proliferating cells but retrieval from the surface in contact-inhibited barrier-forming cells. Fluorescence microscopy experiments showed that in single, contact-devoid cells, TRPC4 resides predominantly in intracellular compartments and is recruited into plasma membrane regions upon formation of cell-cell contacts. Our concept of phenotype-dependent control of TRPC4 targeting and function is illustrated in Fig. 8. Live cell imaging of cells expressing fluorescent fusion proteins confirmed that TRPC4 is recruited specifically into cell-cell junctions. However, we did not detect further recruitment into plasma membrane regions when the cells were stimulated with EGF. EGF-induced promotion of surface expression therefore may not reflect trafficking from deeper intracellular compartments to the plasma membrane but rather insertion of proteins into the plasma membrane from already closely associated membrane structures.

Phenotype dependence was observed not only for TRPC4 targeting but also for agonist-induced Ca^{2+} entry. Three cellular states were distinguished. Single endothelial cells that adopt a migrating state showed the lowest levels of EGF-induced Ca^{2+} entry along with predominant intracellular localization of TRPC4. By contrast, proliferating clusters as well as quiescent, barrier-forming cells displayed both significant levels surface expression of TRPC4 and Ca^{2+} entry. Nonetheless, functional analysis of the contribution of TRPC4 to stimulated Ca^{2+} entry revealed a phenotype-dependent Ca^{2+} entry function of TRPC4 that was not correlated with membrane recruitment. Exclusively in proliferating clusters, which formed immature junctions, was a contribution of TPC4 to EGF-stimulated Ca^{2+} entry evident. Hence, TRPC4 apparently forms distinct signaling complexes in cells of different phenotype. This concept (Fig. 8) was corroborated by the finding that EGF effects on membrane presentation as well as association of TRPC4 with junctional proteins varied with endothelial phenotype. The phenomenon of a tight phenotype-dependent control of this endothelial Ca^{2+} entry system represents a potentially important mechanism for the control of growth factor signaling during tissue development. Tuning of EGF signaling by epithelial cell transitions from a proliferating to a quiescent state via a cell-cell contact-dependent mechanism has recently been suggested (31). Indeed, switching from a contact-uninhibited proliferating to a contact-inhibited state prevented EGF-induced membrane targeting and channel function of TRPC4.

TRPC4 Functions as an Endothelial Ca^{2+} Entry Channel Preferentially in Contact-forming Proliferating Cells—Our results identify TRPC4 as a highly phenotype-dependent endothelial signaling molecule. Genetic knockdown of TRPC4 was without impact on global endothelial Ca^{2+} signaling of single HMEC-1 adopting a migrating state as well as of cells within a contact-inhibited barrier. Only when cells formed initial contacts within proliferating cell clusters, was global endothelial Ca^{2+} signaling sensitive to genetic suppression of TRPC4. Exclusively in proliferating cells, EGF was able to enhance surface presentation of TRPC4. It is tempting to speculate that particular assembly of TRPC4 signaling complexes enables efficient recruitment of channels by EGF. Reorganization of TRPC4 complexes associated with the transition into a mature, barrier-forming endothelial state is likely to favor rapid removal of the channel from the plasma membrane (Fig. 8), as suggested by our surface biotinylation experiments.

Our results complement the findings of a recent study that identified Orai1 rather than TRPC4 as a common and prominent store-operated Ca^{2+} entry channel in single endothelial cells (5). EGF-induced stimulation of phospholipase C initiates both the store-operated Stim/Orai pathway and store-independent activation of TRPC4. Hence, the two mechanisms may contribute at a variable proportion to overall EGF-induced Ca^{2+} entry into endothelial cells of different phenotype. It is of note that store-operated Ca^{2+} entry may involve a cross-talk between Stim/Orai and TRPC signaling, as recently suggested (27–29). The contribution of such a cross-talk to EGF-induced, TRPC4-mediated Ca^{2+} entry into endothelial cells remains to be clarified. Nonetheless, our results unequivocally demonstrate that TRPC4 constitutes a key Ca^{2+} entry pathway in proliferating endothelial cells. This is consistent with the recent documentation of an essential role of TRPC4 in endothelial proliferation. We suggest that the impact of TRPC4 on endothelial proliferation is due to a phenotype-associated Ca^{2+} signaling function.

Localization of TRPC4 within cell-cell contacts is well in line with its suggested role as a determinant of endothelial barrier integrity (3). TRPC4 was shown to play a key role in agonist-induced increase of vascular permeability, which has been attributed to Ca^{2+} influx and $[Ca^{2+}]_i$-induced leakiness of endothelial junctions (30). Because EGF barely generated global Ca^{2+} signals in contact-inhibited, barrier-forming HMEC-1, it is tempting to hypothesize that TRPC4 channels are capable of generating a localized, spatially limited rather than a global, cellular Ca^{2+} signal. Alternatively, TRPC4 may control junctional stability and barrier function by another, as yet unidentified, Ca^{2+} transport-independent mechanism.

Signaling Function of Endothelial TRPC4 Is Governed by Interaction with β-Catenin—TRPC4 was found to be capable of adopting different functional states, corresponding to a fully functional state in proliferating clusters and a state of suppressed functionality in mature barriers. We aimed to identify regulatory interaction partners involved in this phenotype-dependent control of TRPC4 and obtained evidence for interaction of TRPC4 with the junctional proteins β-catenin and VE-cadherin. The observed increase in TRPC4-β-catenin association during stimulation of proliferating cells with EGF prompted us to focus on this as yet unrecognized component of TRPC4 complexes. Further indication for a functional significance of the TRPC4-β-catenin interaction came from our fluorescence microscopy experiments, which showed that β-catenin promoted targeting of TRPC4 in the junctional plasma membrane but intracellular sequestration of the channel in single cells. Overexpression of β-catenin in either HEK293 or HMEC-1 enabled junctional targeting in cell clusters but prevented plasma membrane recruitment of TRPC4 in single cells. Thus, β-catenin interferes with cellular targeting, membrane presentation, and therefore function of the channels (Fig. 8). Evidence for β-catenin-dependent regulation of TRPC4 signaling was also obtained in reconstitution experiments in the HEK293 expression system. Our experiments clearly demonstrate that β-catenin is able to promote TRPC4 function in a cell-cell contact-dependent manner. The previously recognized control of growth factor signaling by β-catenin (13, 31) may be based on cell-cell contact-dependent recruitment of TRPC4 and/or regulatory interactions between TRPC4 and β-catenin. Our results indicate that TRPC4 and β-catenin localize in close proximity within specific junctional complexes of proliferating endothelial cells (see Fig. 8). Involvement of additional scaffold proteins in the interaction between these proteins cannot be excluded at present. Because both TRPC4 and β-catenin contain PDZ interaction domains (6, 32), PDZ scaffolds, such as NHERF (EBP50), a known complex partner of TRPC4 (6), appear as potential molecular linkers in this interaction. Our results prompt further investigations to ultimately resolve the complex composition of the functional endothelial TRPC4 channel complex, which is present in cell-cell contacts and likely to contain further regulatory components. Because β-catenin is a versatile signaling molecule implicated in multiple cellular signaling processes, including transcriptional control of gene expression (33), TRPC4 may be considered as an unrecognized player in β-catenin-dependent pathways, such as Wnt signaling.

Taken together, our investigations provide evidence for novel as yet unrecognized signaling functions of a TRPC channel. We introduce TRPC4 as a cell-cell contact-dependent endothelial Ca^{2+} entry channel and as a potential player in the β-catenin signaling network. In view of the strictly cell state-dependent membrane recruitment and function of TRPC4, the role of this channel in endothelial Ca^{2+} homeostasis needs to be reconciled. TRPC4 emerges as a player that is able to complement or replace other Ca^{2+} entry systems specifically during endothelial phenotype transitions.

Acknowledgments—We thank Dr. V. Flockerzi for kindly providing anti-TRPC4-antibody, Dr. R. M. Kypta for providing β-catenin cDNA, and Dr. F. Candal for making the HMEC-1 cell line available. We also thank Renate Schmidt for excellent technical assistance.

REFERENCES

1. Wakabayashi, I., Poteser, M., and Groschner, K. (2006) *J. Vasc. Res.* **43,** 238–250
2. Freichel, M., Suh, S. H., Pfeifer, A., Schweig, U., Trost, C., Weissgerber, P., Biel, M., Philipp, S., Freise, D., Droogmans, G., Hofmann, F., Flockerzi, V., and Nilius, B. (2001) *Nat. Cell Biol.* **3,** 121–127

3. Tiruppathi, C., Freichel, M., Vogel, S. M., Paria, B. C., Mehta, D., Flockerzi, V., and Malik, A. B. (2002) *Circ. Res.* **91,** 70–76
4. Cioffi, D. L., and Stevens, T. (2006) *Microcirculation* **13,** 709–723
5. Abdullaev, I. F., Bisaillon, J. M., Potier, M., Gonzalez, J. C., Motiani, R. K., and Trebak, M. (2008) *Circ. Res.* **103,** 1289–1299
6. Mery, L., Strauss, B., Dufour, J. F., Krause, K. H., and Hoth, M. (2002) *J. Cell Sci.* **115,** 3497–3508
7. Corada, M., Liao, F., Lindgren, M., Lampugnani, M. G., Breviario, F., Frank, R., Muller, W. A., Hicklin, D. J., Bohlen, P., and Dejana, E. (2001) *Blood* **97,** 1679–1684
8. Lampugnani, M. G., and Dejana, E. (1997) *Curr. Opin. Cell Biol.* **9,** 674–682
9. Dejana, E., Orsenigo, F., Molendini, C., Baluk, P., and McDonald, D. M. (2009) *Cell Tissue Res.* **335,** 17–25
10. Navarro, P., Caveda, L., Breviario, F., Mândoteanu, I., Lampugnani, M. G., and Dejana, E. (1995) *J. Biol. Chem.* **270,** 30965–30972
11. Vestweber, D. (2000) *J. Pathol.* **190,** 281–291
12. Vestweber, D. (2008) *Arterioscler. Thromb. Vasc. Biol.* **28,** 223–232
13. Kim, K. I., Cho, H. J., Hahn, J. Y., Kim, T. Y., Park, K. W., Koo, B. K., Shin, C. S., Kim, C. H., Oh, B. H., Lee, M. M., Park, Y. B., and Kim, H. S. (2006) *Arterioscler. Thromb. Vasc. Biol.* **26,** 91–98
14. Heupel, W. M., Efthymiadis, A., Schlegel, N., Müller, T., Baumer, Y., Baumgartner, W., Drenckhahn, D., and Waschke, J. (2009) *J. Cell Sci.* **122,** 1616–1625
15. Schindl, R., Frischauf, I., Kahr, H., Fritsch, R., Krenn, M., Derndl, A., Vales, E., Muik, M., Derler, I., Groschner, K., and Romanin, C. (2008) *Cell Calcium* **43,** 260–269
16. Zimmermann, T. (2005) *Adv. Biochem. Eng. Biotechnol.* **95,** 245–265
17. Zimmermann, T., Rietdorf, J., and Pepperkok, R. (2003) *FEBS Lett.* **546,** 87–92
18. Flockerzi, V., Jung, C., Aberle, T., Meissner, M., Freichel, M., Philipp, S. E., Nastainczyk, W., Maurer, P., and Zimmermann, R. (2005) *Pflugers Arch.* **451,** 81–86
19. Giannini, A. L., Vivanco, M., and Kypta, R. M. (2000) *J. Biol. Chem.* **275,** 21883–21888
20. Giannini, A. L., Vivanco, M. M., and Kypta, R. M. (2000) *Exp. Cell Res.* **255,** 207–220
21. Kamei, J., Toyofuku, T., and Hori, M. (2003) *Biochem. Biophys. Res. Commun.* **312,** 380–387
22. Kuang, H. B., Miao, C. L., Guo, W. X., Peng, S., Cao, Y. J., and Duan, E. K. (2009) *Front. Biosci.* **14,** 2212–2220
23. Poteser, M., Graziani, A., Rosker, C., Eder, P., Derler, I., Kahr, H., Zhu, M. X., Romanin, C., and Groschner, K. (2006) *J. Biol. Chem.* **281,** 13588–13595
24. Schindl, R., Frischauf, I., Kahr, H., Fritsch, R., Krenn, M., Derndl, A., Vales, E., Muik, M., Derler, I., Groschner, K., and Romanin, C. (2008) *Cell Calcium* **43,** 260–269
25. Odell, A. F., Van Helden, D. F., and Scott, J. L. (2008) *J. Biol. Chem.* **283,** 4395–4407
26. Odell, A. F., Scott, J. L., and Van Helden, D. F. (2005) *J. Biol. Chem.* **280,** 37974–37987
27. Liao, Y., Erxleben, C., Yildirim, E., Abramowitz, J., Armstrong, D. L., and Birnbaumer, L. (2007) *Proc. Natl. Acad. Sci. U.S.A.* **104,** 4682–4687
28. Cheng, K. T., Liu, X., Ong, H. L., and Ambudkar, I. S. (2008) *J. Biol. Chem.* **283,** 12935–12940
29. Kim, M. S., Zeng, W., Yuan, J. P., Shin, D. M., Worley, P. F., and Muallem, S. (2009) *J. Biol. Chem.* **284,** 9733–9741
30. Tiruppathi, C., Ahmmed, G. U., Vogel, S. M., and Malik, A. B. (2006) *Microcirculation* **13,** 693–708
31. Kim, J. H., Kushiro, K., Graham, N. A., and Asthagiri, A. R. (2009) *Proc. Natl. Acad. Sci. U.S.A.* **106,** 11149–11153
32. Theisen, C. S., Wahl, J. K., 3rd, Johnson, K. R., and Wheelock, M. J. (2007) *Mol. Biol. Cell* **18,** 1220–1232
33. Masckauchán, T. N., Shawber, C. J., Funahashi, Y., Li, C. M., and Kitajewski, J. (2005) *Angiogenesis* **8,** 43–51